




The electrochemical fabrication of hydrogels: a short review

Emily R. Cross¹ 

Received: 22 October 2019 / Accepted: 5 February 2020 / Published online: 13 February 2020

© The Author(s) 2020 

Abstract

Electrochemical hydrogel fabrication is the process of preparing hydrogels directly on to an electrode surface. There are a variety of methods to fabricate hydrogels, which are specific to the type of gelator and the desired properties of the hydrogel. A range of analytical methods that can track this gelation and characterise the final properties are discussed in this short review.

Keywords Hydrogel · Fabrication · Biofabrication · Electrogelation

1 Introduction

Electrochemical hydrogel fabrication is a common term used to describe the process of preparing hydrogels on to an electrode surface. However, other phrases such as electrodeposition, bio-assembly, bio-printing, e-gels and electrogelation are also used to describe this process. Hydrogels can be prepared by changing the solubility of the gelating component on the electrode surface [1–3]. There are a variety of reduction and oxidation (redox) methods used to induce this change in solubility. Commonly, methods are chosen considering a combination of the gelator type, solution composition and the desired properties of the final product. These methods require either the reduction or oxidation of a species in the gelator solution (Table 1).

Although the methods to fabricate hydrogels on an electrode surface may differ, the fundamental principles are similar. In general, these methods create a solubility gradient in which the gelator is soluble in the bulk solution but insoluble at the electrode surface. This change in solubility triggers the assembly of gelator components into hydrogels on the electrode surface, while in the bulk solution the gelator components remain soluble. Figure 1 shows how redox trigger hydroquinone can be oxidised on

an electrode surface, producing benzoquinone and protons. The protons set up a pH gradient which is low on the electrode surface and high in the bulk solution [2, 11]. The resulting low pH triggers gel formation which continues to grow as the hydroquinone is continuously oxidised.

Common electrochemical set ups include a working electrode such as a glassy carbon, platinum, or FTO (fluorine doped tin oxide)/ITO (indium doped tin oxide) coated glass, within a three-electrode system. Electrode surfaces can be patterned in order for a hydrogel of a specific shape to be prepared (see Sect. 2.1). Electrode pens have the advantage of being mobile and can be used to sketch regions within a bulk gelator solution. The sketched regions are less soluble than the bulk which triggers the self-assembly of the gelator [30]. Gelation by an electrode pen allows for greater spatial control within a bulk solution than regular triggers. Affixing an electrode pen to a mechanical arm allows for programmed 3-dimensional printing of hydrogels. Figure 2 shows examples of both stationary and mobile electrochemical fabrication techniques.

Recent advances in potentiostat production have made potentiostats available which are small, do-it-yourself, portable and cheap allowing for greater access for fabrication techniques [31–34]. This review will discuss some of

✉ Emily R. Cross, e.cross.1@research.gla.ac.uk | ¹School of Chemistry, University of Glasgow, Glasgow, UK.



Table 1 Methods for electrochemical hydrogel fabrication

Redox triggers	Gelator	References
<i>Oxidation</i>		
Water oxidation	Silk	[4–8]
	Alginic acid	[9]
	Hyaluronic acid	[10]
Hydroquinone (forms benzoquinone and H ⁺)	Low molecular weight gelators (–COOH terminus)	[2, 11, 12]
Fe(II) (forms Fe ³⁺)	Alginate	[13]
	Poly acrylic acid	[14]
Catechol (forms quinone)	Polyallylamine hydrochloride	[15, 16]
Cu (0) (forms Cu ²⁺)	Chitosan	[17]
	Carboxymethylcellulose	[18]
Cl ₂	Putative crosslinking of chitosan	[19]
Enzymes	Covalent crosslinking specific to enzyme type	[20, 21]
<i>Reduction</i>		
Water reduction	Collagen	[22, 23]
	Chitosan	[3, 24–28]
Ruthenium complex [Ru(bpy) ₂]Cl ₂	Chitosan	[29]

Fig. 1 Image of a gel growing on a glassy carbon electrode as a fixed current is applied over time. **R** represents the redox trigger diffusing to the electrode surface, reacting to form a product, **P**, which triggers gelation. The volume of the gel on the surface increases with time. Figure from unpublished data

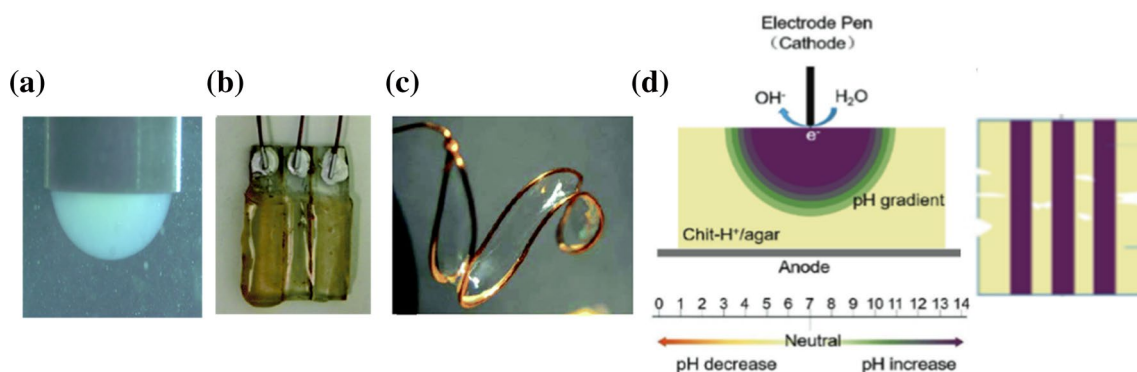
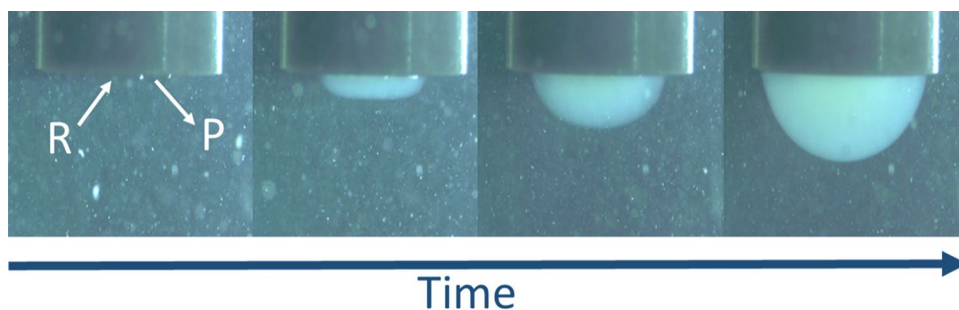


Fig. 2 **a** Low molecular weight hydrogel grown on a glassy carbon electrode. **b** Low molecular weight hydrogel grown on a FTO glass electrode, reproduced from Ref. [11] with permission from The Royal Society of Chemistry. **c** Three-dimensional silk gel grown on a copper wire electrode, reproduced from Ref. [7] with permission from The Royal Society of Chemistry. **d** Schematic diagram

of: left, an electrode pen dipping into the surface of a bulk solution containing protonated chitosan and agar causing electrolysis, an increase in pH and subsequently chitosan gel formation; right, the resulting sketched line regions of chitosan gel surrounded by the bulk solution. Reproduced from Ref. [30] with permission from ©2018 WILEY-VCH Verlag GmbH & Co. KGaA, Weinheim

the challenges that are shared between electrochemical hydrogel fabrication methods and how these have been

addressed. The methods used to analyse gels will also be highlighted.

1.1 Applications of electrochemically fabricated hydrogels

Electrochemical hydrogel fabrication provides new opportunities for constructing at the micro- and nanoscale [35, 36]. Unlike gels formed in bulk which take the shape of the container they are poured into when liquid, electrochemically fabricated hydrogels can be formed on any conductive surface which provides a high level of spatiotemporal control. Gels can then be used to encapsulate enzymes, nanomaterials, drugs or cells as shown in Fig. 3 [37]. The potential for new opportunities for constructing at the micro- and nano-scale is attracting increasing attention in a large range of potential applications, including synthesis of conducting polymers [38]; for use in regenerative medicine [39, 40]; and the rapidly growing field of biosensors and microfluidic devices [41–45]; Electrochemically fabricated hydrogels can also be used to create antibacterial surfaces [46] and the coating of medical implants [47, 48].

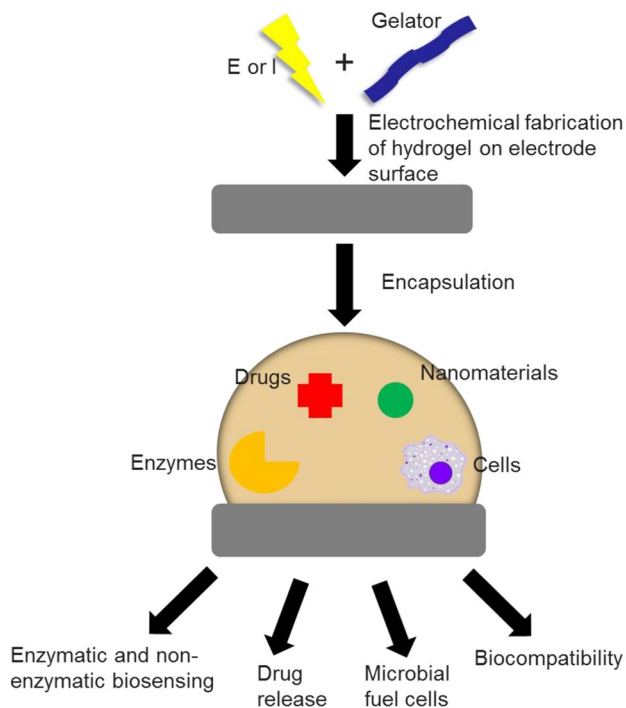


Fig. 3 Schematic representation of the process for electrochemical fabrication of hydrogels. Allowing the encapsulation of enzymes, drugs, nanomaterials, or cells, these processes are applied in several applications, such as biosensors [41–44], corrosion prevention [49], antimicrobial coatings, drug-release [50], barrier properties and cell encapsulation [45]

2 Biological versus synthetic

There are a wide range of gelators that can be used to form hydrogels on an electrode surface. These include synthetic gelators and materials deriving from biological sources [12]. Chitosan was the first biopolymer to be formed on an electrode surface [51]. When using gelators originating from biological sources, there can be issues of batch-to-batch variation such as inconsistencies in molecular weight, purity and possible contamination. All of these can mean that the final hydrogels have irreproducible properties. Other production-related issues with the use of chitosan produced from shellfish is the seasonality of the industrial harvest. When using naturally-occurring chitosan, there is also a significant risk of reticent anaphylaxis which limits clinical use [52]. Purified biologically-sourced gelators can of course be formed but this comes at an inflated cost.

Synthetic gelators can be used to mimic biological materials [53, 54]. These materials are usually based on covalently cross-linked polymer networks such as TrueGel3D™, Hystem® and HydroMatrix™. Other synthetic hydrogels are held together with only physical interactions without the need for covalent cross linkers, such as low molecular weight gelators [55–57]. These gelators form reproducible gels in both the bulk [58], and fabricated on an electrode [11]. Hydrogels formed using low molecular weight gelators can also be converted into polymers on an electrode [38]. The biocompatibility of hydrogels formed from synthetic gelators can be somewhat challenging. In order for the gels to be used in cell culture, they must be formed at a compatible pH (generally physiological pH) and cannot contain any materials that would induce cell death. Forming gels at physiological pH is difficult with certain pH triggered methods as they usually results in gels with high or too low a pH [2].

For biological applications, both biologically derived and synthetic gels are often required to be placed in pH buffered cell media. The contents of cell media can include a mixture of glucose, antibiotics and buffered salt solutions. It is necessary therefore to test whether the effect of leaving the gels in a buffered solution affects the properties which we aim to control electrochemically.

2.1 Spatiotemporal control

Spatiotemporal control is the term used to describe the fabrication of a gel by controlling the parameters of time and space, such as controlling the rate of growth and the resulting size and thickness of the gel.

Hydrogels can be prepared on a range of electrode surfaces with any geometry, within a stationary electrode system, they can also be sketched, or printed using a mobile electrode pen [30, 59]. Stationary electrodes can be any shape and size on any length scale with the desired gel forming on the surface [1, 60, 61]. Conductive glass electrodes such as ITO and FTO can be etched to allow for regions of conductive/non-conductive areas [11], which results in gels only forming on the conductive regions [2, 11]. As well as forming gels in a two-dimensional plane, three-dimensional gels can be formed by simply bending a two-dimensional electrode into an additional plane [7]. Bressner et al. [7] showed a bent copper wire forming a closed loop electrode could be used to prepare the first electro fabrication of silk gels in three-dimensions. Photocathodes can also be used to produce patterned gels. The photocathodes selectively produce electrode surface reactions. Jiang and co-workers controlled the illumination pattern on a digital micro-mirror device in order to produce chitosan gels with difference shaped and sizes and as well as multiplexed micro-patterning [62].

Electrode pens can be formed from a variety of conductive materials and sizes. Su et al. formed a cathodic electrode pen from a stainless-steel acupuncture needle. The pen once placed on the surface of a bulk gelator solution can create regions where gelation is triggered. The writing speed and holding time can determine the thickness of the gels formed [30]. Figure 4 shows examples of the spatial temporal control from both stationary and mobile electrodes [18, 30].

Further spatiotemporal control can be achieved by controlling the electrical input to the electrode. Yan et al. have shown the formation of chitosan on a glassy carbon electrode can be controlled by oscillating electrical signals. This oscillation in electrical signal enables segmented structures to be generated, which are consistent with the clock and wavefront framework [63]. Controlling the electrical signals also allows for the sequential assembly of gelators. This can be applied to multicomponent gelators systems on the same electrode. Controlling the applied current can selectively trigger individual gelators within multicomponent systems as Raeburn et al. [11] have shown for pH triggered gelators of differing pK_a values. Layered structures can also be prepared on separate electrodes within the same system as demonstrated by Wang et al. [64]. Sequential assembly of gels is of particular interest for microfluidic channels for lab-on-a-chip applications [64], and for use as conductive materials.

2.2 Homogeneity

In order to form reproducible gels, there needs to be homogeneity within gel phases [58]. This can be difficult to analyse. Fabrication methods which produce gas on the electrode surface may form bubbles within the gel or leave holes where the gas has diffused out. This can compromise mechanical stiffness, gel clarity and can act as an electrical insulator that slows down continued gel formation [7, 65]. A camera can be used to analyse the size and distribution of the bubbles within the gel which can keep track of bubbles forming and analyse the size of the gel [2]. Kaplan and Migliaresi have both shown how the rate of bubble formation can be minimised by regulating the current within solution [5, 65].

2.3 Removing the gel from the electrode surface

In the cases where the gels do not form any chemical bonds to the electrode surface, they can be removed by gently tapping or scraping the gel from the surface [7]. In addition, there are methods which can remove gels from a surface remotely. These methods either reduce the solubility of the gelator at the electrode surface and gel interface [66], or by producing a gas which pushes the gel off of the electrode [61]. This can be done by reversing the applied current [65]. Payne and co-workers have shown how pH switch gels formed by the reduction of water can be removed from the surface of the electrode by reversing the potential where the oxidation of water occurs causing acidification. This induced acidification of chitosan gels can induce multilayer disassembly [67]. Potential reversal has also been used to remove gels from a patterned micro-electrode surface as shown in Fig. 5 [61].

3 Gel growth analysis

3.1 pH determination

Measuring the pH during gelation is important for pH triggered gels as the rate of pH change determines the rate of gelation [30]. As gelation occurs once the pH has passed the pK_a of a pH-triggered gelator [68], the rate of pH change controls the rate of gelation which can yield gels of different physical properties [69].

It is difficult to measure the pH of a gel or the bulk solution when a current is flowing, as the current interferes with the moving ions in the pH electrode tip. Although this can provide pH data with a range of error depending upon the concentration of ions in solution, the pH values are still usually reported. pH indicators such as universal indicator and methyl red can be added

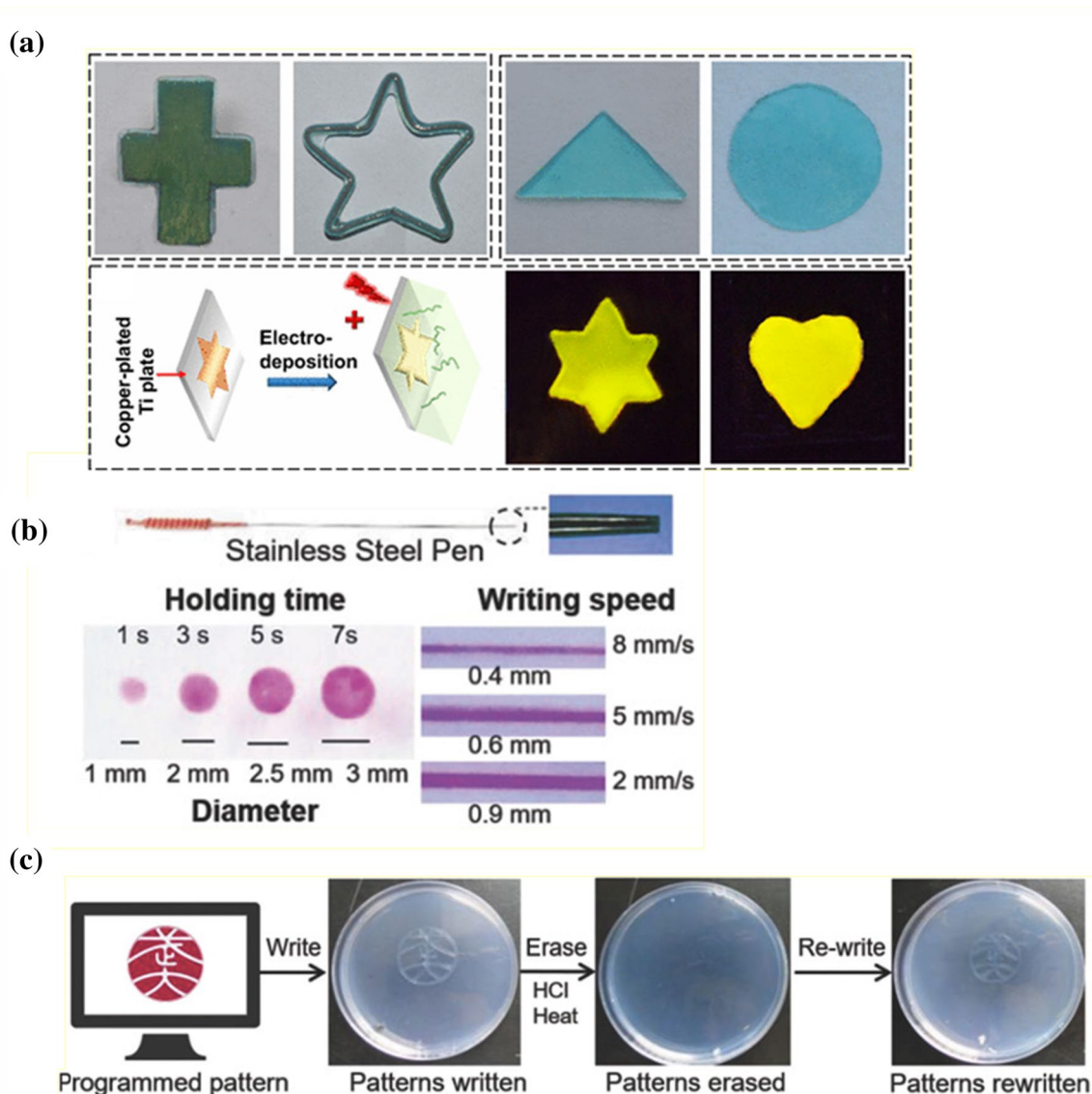


Fig. 4 a i) images of deposited films on a copper plate and copper wire electrodes, ii) images of deposited films with different shapes detached from copper plates. Iii) schematic illustration for fabricating fluorescence patterns on the deposited film on a copper-plated titanium plate, and images of the fluorescence patterns under 254 nm UV light. All images for **a** were reprinted by permission from Springer: Springer, Cellulose, [18] © 2018. **b** Cathodic writing

on a chitosan/agarose hydrogel using a stainless-steel pen electrode. The longer holding times result with a gel of a larger area. The slower writing speed produces gels with greater thickness. **c** A programmed pattern written onto the gel surface which can be erased and rewritten. Both **b** and **c** are reprinted by permission from ©2018 WILEY-VCH Verlag GmbH & Co. KGaA, Weinheim

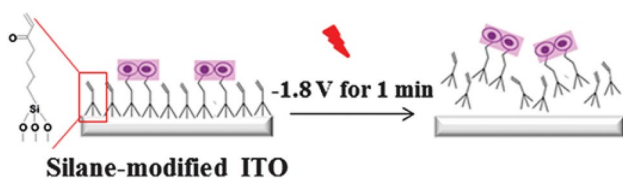


Fig. 5 Electrochemical detachment of HepG2 cells inside herapin based hydrogels from a modified ITO electrode. Electrochemical detachment was triggered by a negative potential of -1.8 V being applied for 1 min. Reproduced from Ref. [61] with permission from The Royal Society of Chemistry

to the gelator solution which changes colour as the pH is changed [7, 8]. This can provide a simple approach to determine areas of different pH. Using an indicator is useful for measuring parts of the gel visible by the human eye or by spectrometry. However, to the best of our knowledge, a method to determine the exact pH at the electrode and gel interface during gelation has not been identified.

4 Optical imaging of electrofabricated hydrogels

In situ imaging is an essential tool to analyse gel growth. Images can be used to analyse the rate of gel growth and determine the shape and size of the gel [1, 2, 11, 63]. As the development of mobile phone camera resolution has progressed, in some cases a phone camera is all that is needed to record rate of gel growth, shape and area. Open source software such as ImageJ can be used to trace the outline of the gel on the electrode surface and calculates its area as well as analysing any bubble formation in the gel (Fig. 6) [70].

5 Nuclear magnetic resonance (NMR)

Advances in in situ analysis techniques for gelation such as NMR [71–73] have limited use in electrochemical gels due to the inability to physically apply the methods. Wallace et al. [71–73] have shown how NMR can be used to determine the gelator pK_a and pore size in bulk gelation. Development of these techniques for an electrochemical system would allow for greater analysis of gelation

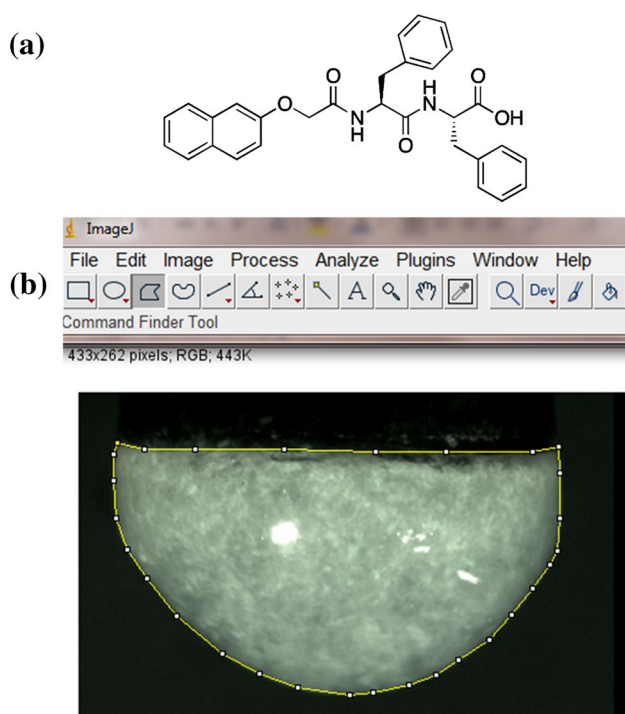


Fig. 6 **a** Low molecular weight gelator that is fabricated on a glassy carbon electrode. **b** Gel formed from gelator in **a** on a glassy carbon electrode. ImageJ software is used to trace around the gel area to determine its volume

kinetics. For gels formed on an electrode, the self-assembly process can be followed by NMR visible gelator molecules e.g. approximately smaller than 25 kDa [74]. Large gelators experience slow tumbling in solution which leads to faster relaxation of transverse magnetisation, this causes the gelator to appear invisible in the spectra [74]. NMR self-assembly analysis involves removing the gel from the electrode surface at different time points during gelation, freeze drying the gels then placing in a deuterated solvent and analysed using NMR spectroscopy. The NMR peaks are then integrated against a known standard to determine

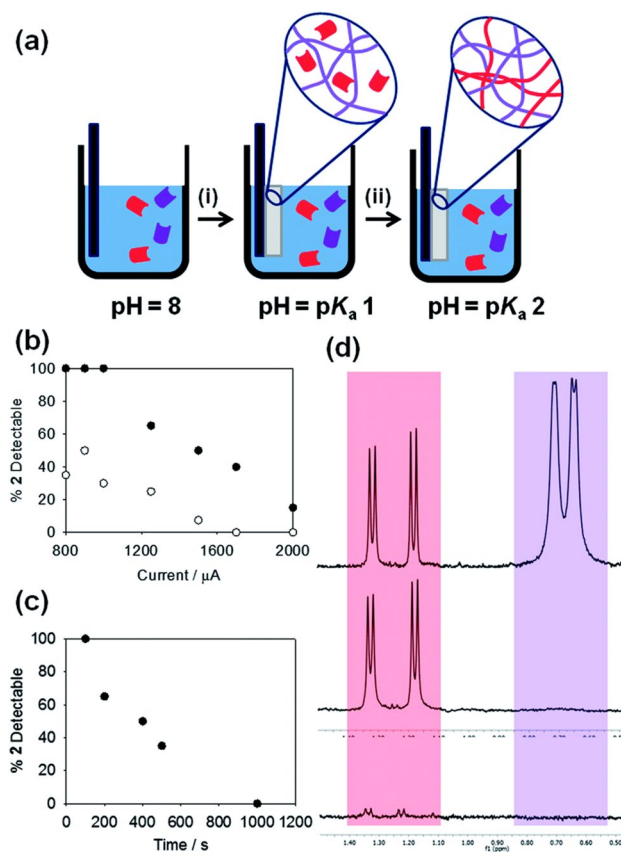


Fig. 7 **a** Schematic showing the sequential assembly of two gelators in a multi-component system. (i) The gelator with the highest pK_a will assemble first as the pH is decreased, whilst the second gelator will remain in solution until (ii) its pK_a is reached. **b** Percentage of the gelator with the highest pK_a (**1**) detectable in the NMR spectrum of a gelled 1:1 mixture the two gelators; gels formed at different currents for times of (black circles) 100 s and (White circles) 300 s. **c** Percentage of gelator with the lower pK_a (**2**) detectable in the NMR spectrum of a gelled 1:1 mixture of both gelators; gels formed at a current of 800 mA for different times. **d** Partial NMR spectra for (top) stock solution of both gelators, the purple peaks are from the gelator **1** and the red peaks are gelator **2**; (middle) application of a current of 1250 mA for 100 s results in loss of the peaks from **1** whilst **2** remains in solution; (bottom) application of a current of 2000 mA for 300 s results in the loss of peaks from both **1** and **2**, showing that both have gelled. Reproduced from Ref. [11] with permission from The Royal Society of Chemistry

gelator concentration. [11, 75]. Following the self-assembly during gelation allows for the content of the gel to be identified, which is of particular use for multicomponent systems as shown in Fig. 7.

5.1 Gel property analysis

This section will evaluate how electrochemical fabricated gels are currently analysed. In order to analyse gels, the techniques must not distort the physical properties of the material [76]. An ideal method for gel analysis must have the following characteristics:

- Represent the three-dimensional hydrogel, not just the surface.
- Be a process that does not require environmental conditions that modify the materials morphology to an unknown degree e.g. cryogenically freezing, swelling, pressure changes or placing in a salt buffered solution.
- Have a sample preparation process that does not alter the matrix or self-assembly process e.g. avoid methods where samples are manually cut after freezing, coated in gold, or the addition of probe particles.

If these conditions are not met, analysis results can end up inaccurate. For example, Mears et al. showed how the drying of gels can affect the structural network. Comparing the fibre width of a low molecular weight gel using scanning electron microscopy (SEM), cryo-transmission electron microscopy (cryo-TEM) and small angle neutron scattering (SANS) measurements and revealed how the fibre widths differed between gels that were hydrated and dried [77].

5.2 Characterisation of hydrogel nano/microstructures

Electron imaging techniques such as SEM or TEM can produce images of dried gel surfaces to reveal the morphologies of micelles, polymers and the overlapping of fibres [78]. From these images, the analysis of fibre width, length and pore size are often acquired. Three-dimensional images can be obtained by cryogenically freezing the gels then fracturing the matrix to reveal a cross section [79]. However, the disadvantages of using SEM, TEM and other in situ techniques include the vacuuming or cryogenically freezing of the gels. The collapsing of the matrix due to vacuum and the expansion of the matrix due to water freezing can dramatically modify the gels morphology making it difficult to make accurate quantitative analysis of the gels without an unknown degree of error [77]. However, SEM imaging can be useful to qualitatively

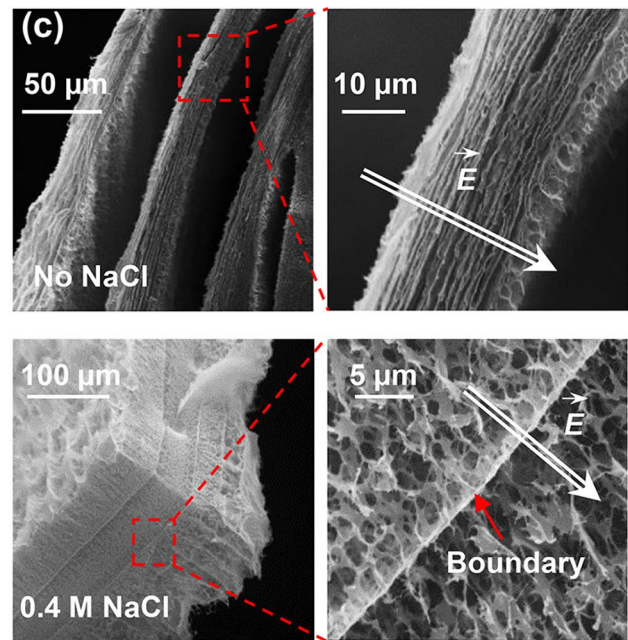


Fig. 8 SEM images of segmented chitosan hydrogels show aligned segments for gels deposited in the absence of NaCl, while gels deposited in the presence of salt show porous random structures. Arrows indicate electric field. Adapted with permission from [63]. Copyright 2018 American Chemical Society

analyse different structural regions within a gel as shown in Fig. 8 [63].

Quantitative polarised light microscopy (qPLM) can be used to identify microstructural organisation within fabricated gels. Yan et al. used Brillouin spectroscopy to show how gradients in mechanical properties and differences within internal patterns can be identified during and after gelation. By combining both qPLM and Brillouin spectroscopy, they were able to clarify the mechanisms responsible for the emergence of segmented structure during chitosan's electrodeposition (Fig. 9).

5.3 Diffraction

Conventional X-ray diffraction generally gives broad, amorphous patterns for gels meaning that analysis is difficult. However, it can be a useful technique to identify fabricated crystalline structures within an amorphous gel such as chitosan's self-assembly into crystals [30]. Small angle scattering can be used to analyse gel properties such as fibre length, shape, fractional dimensions, alignment and size. Small angle scattering can be applied on many length scales ranging from 0.1 to 1000 nm which can be combined to observe a large range [80]. In bulk gelation, contrast matching of gel fibres can be used to differentiate different components within a multicomponent system [69]. This can be used to determine if fibres are composed

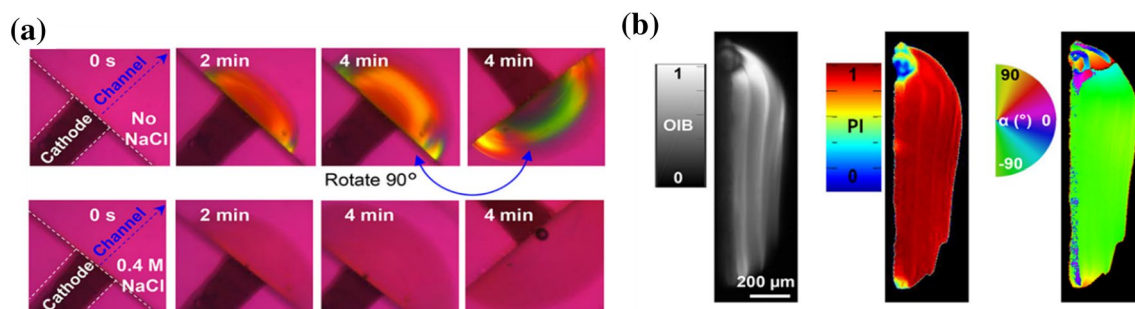


Fig. 9 Electrical control of emerging nanostructures. **a** Time lapse images that show gels deposited in the absence of NaCl are birefringent whereas gels deposited in the presence of NaCl show little birefringence. **b** Quantitative polarised light microscopy metrics of

orientation-independent birefringence, parallelism index, and local optical axis orientation of chitosan electrodeposited in the absence of salt. Adapted with permission from [63]. Copyright 2018 American Chemical Society

of self-sorted or co-sorted gelators [69]. Methods such as these would be useful to analyse electrochemical gelation.

5.4 Rheology

Oscillatory rheology can be used to determine homogeneity, stiffness and strength of a gel [30]. Si et al. used a rheological approach, tensiometry to show how the mechanical properties of a chitosan gel were enhanced by using a cathodic writing pen versus a chitosan gel that was unwritten [30].

Rheology is an extremely useful tool for biofabricated gels. The stiffness of the gels amongst other factors controls the differentiation pathway of stem cells into tissue [81]. For those with a biology background, rheology data is usually provided giving the Young's modulus, whereas a chemical/engineering background usually provides the storage and loss moduli which can cause some confusion. However, the relationship between the two is relatively simple and shown in Eqs. 1 and 2.

$$E = G^*(2\nu + 1) \quad (1)$$

$$G^* = G' + iG'' \quad (2)$$

where E represents Young's modulus, G^* the complex modulus, ν the Poisson ratio which is usually 0.5 for a hydrogel [82], i the imaginary component, G' the storage modulus and G'' the loss modulus.

6 Conclusion

The past decade has seen a rise in electrochemical fabrication developments such as advances in spatiotemporal control, gelator development, and the identification of new fabrication methods. These advances may provide a

way to achieve an ethical, reproducible and accurate biological cell model such as representing the blood brain barrier where other bulk gels have failed. Improvements in existing and the development of new analytical methods of gel characterisation as well as the improvement in the methods accessibility will allow scientists from all backgrounds to communicate their research more accurately and efficiently, propelling the field from bench to market in the not so distant future.

Acknowledgements ERC thanks the University of Glasgow for a studentship.

Compliance with ethical standards

Conflict of interest There are no conflicts to declare.

Open Access This article is licensed under a Creative Commons Attribution 4.0 International License, which permits use, sharing, adaptation, distribution and reproduction in any medium or format, as long as you give appropriate credit to the original author(s) and the source, provide a link to the Creative Commons licence, and indicate if changes were made. The images or other third party material in this article are included in the article's Creative Commons licence, unless indicated otherwise in a credit line to the material. If material is not included in the article's Creative Commons licence and your intended use is not permitted by statutory regulation or exceeds the permitted use, you will need to obtain permission directly from the copyright holder. To view a copy of this licence, visit <http://creativecommons.org/licenses/by/4.0/>.

References

1. Fernandes R, Wu L-Q, Chen T, Yi H, Rubloff GW, Ghodssi R, Bentley WE, Payne GF (2003) Electrochemically induced deposition of a polysaccharide hydrogel onto a patterned surface. *Langmuir* 19:4058–4062
2. Johnson EK, Adams DJ, Cameron PJ (2010) Directed self-assembly of dipeptides to form ultrathin hydrogel membranes. *J Am Chem Soc* 132:5130–5136

3. Pang X, Zhitomirsky I (2005) Electrodeposition of composite hydroxyapatite–chitosan films. *Mater Chem Phys* 94:245–251
4. Lu Q, Huang Y, Li M, Zuo B, Lu S, Wang J, Zhu H, Kaplan DL (2011) Silk fibroin electrogelation mechanisms. *Acta Biomater* 7:2394–2400
5. Maniglio D, Bonani W, Bortoluzzi G, Servoli E, Motta A, Migliaresi C (2010) Electrodeposition of silk fibroin on metal substrates. *J Bioact Compatible Polym* 25:441–454
6. Tabatabai AP, Kaplan DL, Blair DL (2015) Rheology of reconstituted silk fibroin protein gels: the epitome of extreme mechanics. *Soft Matter* 11:756–761
7. Bressner JE, Marelli B, Qin G, Klinker LE, Zhang Y, Kaplan DL, Omenetto FG (2014) Rapid fabrication of silk films with controlled architectures via electrogelation. *J Mater Chem B* 2:4983–4987
8. Kojic N, Panzer MJ, Leisk GG, Raja WK, Kojic M, Kaplan DL (2012) Ion electrodiffusion governs silk electrogelation. *Soft Matter* 8:6897–6905
9. Cheong M, Zhitomirsky I (2008) Electrodeposition of alginate acid and composite films. *Colloids Surf A* 328:73–78
10. Ma R, Epand RF, Zhitomirsky I (2010) Electrodeposition of hyaluronic acid and hyaluronic acid–bovine serum albumin films from aqueous solutions. *Colloids Surf B* 77:279–285
11. Raeburn J, Alston B, Kroeger J, McDonald TO, Howse JR, Cameron PJ, Adams DJ (2014) Electrochemically-triggered spatially and temporally resolved multi-component gels. *Mater Horiz* 1:241–246
12. Johnson EK, Chen L, Kubiak PS, McDonald SF, Adams DJ, Cameron PJ (2013) Surface nucleated growth of dipeptide fibres. *Chem Commun* 49:8698–8700
13. Jin Z, Güven G, Bocharova V, Halánek J, Tokarev I, Minko S, Melman A, Mandler D, Katz E (2012) Electrochemically controlled drug-mimicking protein release from iron–alginate thin-films associated with an electrode. *ACS Appl Mater Interfaces* 4:466–475
14. He S, Ren B, Liu X, Tong Z (2010) Reversible electrogelation in poly(acrylic acid) aqueous solutions triggered by redox reactions of counterions. *Macromol Chem Phys* 211:2497–2502
15. Wu L-Q, Ghodssi R, Elabd YA, Payne GF (2005) Biomimetic pattern transfer. *Adv Funct Mater* 15:189–195
16. Maerten C, Garnier T, Lupattelli P, Chau NTT, Schaaf P, Jierry L, Boulmedais F (2015) Morphogen electrochemically triggered self-construction of polymeric films based on mussel-inspired chemistry. *Langmuir* 31:13385–13393
17. Payne GF, Raghavan SR (2007) Chitosan: a soft interconnect for hierarchical assembly of nano-scale components. *Soft Matter* 3:521–527
18. Wang Y, Zhang Z, Wang M, Guo C, Liu H, Zeng H, Duan X, Zhou Y, Tang Z (2018) Direct electrodeposition of carboxymethyl cellulose based on coordination deposition method. *Cellulose* 25:105–115
19. Gray KM, Liba BD, Wang Y, Cheng Y, Rubloff GW, Bentley WE, Montembault A, Royaud I, David L, Payne GF (2012) Electrodeposition of a biopolymeric hydrogel: potential for one-step protein electroaddressing. *Biomacromolecules* 13:1181–1189
20. Liu Y, Terrell JL, Tsao C-Y, Wu H-C, Javvaji V, Kim E, Cheng Y, Wang Y, Ulijn RV, Raghavan SR, Rubloff GW, Bentley WE, Payne GF (2012) Biofabricating multifunctional soft matter with enzymes and stimuli-responsive materials. *Adv Funct Mater* 22:3004–3012
21. Wang J, Miao X, Fengzhao Q, Ren C, Yang Z, Wang L (2013) Using a mild hydrogelation process to confer stable hybrid hydrogels for enzyme immobilization. *RSC Adv* 3:16739–16746
22. Zhuang J, Lin S, Dong L, Cheng K, Weng W (2018) Magnetically assisted electrodeposition of aligned collagen coatings. *ACS Biomater Sci Eng* 4:1528–1535
23. Ling T, Lin J, Tu J, Liu S, Weng W, Cheng K, Wang H, Du P, Han G (2013) Mineralized collagen coatings formed by electrochemical deposition. *J Mater Sci Mater Med* 24:2709–2718
24. Jiang T, Zhang Z, Zhou Y, Liu Y, Wang Z, Tong H, Shen X, Wang Y (2010) surface functionalization of titanium with chitosan/gelatin via electrophoretic deposition: characterization and cell behavior. *Biomacromolecules* 11:1254–1260
25. He H, Cao X, Dong H, Ma T, Payne GF (2017) Reversible programming of soft matter with reconfigurable mechanical properties. *Adv Funct Mater* 27:1605665
26. Wang F, Huang P, Huang D, Hu Y, Ma K, Cai X, Jiang T (2018) Preparation and functionalization of acetylsalicylic acid loaded chitosan/gelatin membranes from ethanol-based suspensions via electrophoretic deposition. *J Mater Chem B* 6:2304–2314
27. Li Y, Liu Y, Gao T, Zhang B, Song Y, Terrell JL, Barber N, Bentley WE, Takeuchi I, Payne GF, Wang Q (2015) Self-assembly with orthogonal-imposed stimuli to impart structure and confer magnetic function to electrodeposited hydrogels. *ACS Appl Mater Interfaces* 7:10587–10598
28. Pang X, Zhitomirsky I (2008) Electrodeposition of hydroxyapatite–silver–chitosan nanocomposite coatings. *Surf Coat Technol* 202:3815–3821
29. Zhang Y, Ji C (2010) Electro-induced covalent cross-linking of chitosan and formation of chitosan hydrogel films: its application as an enzyme immobilization matrix for use in a phenol sensor. *Anal Chem* 82:5275–5281
30. Wu S, Yan K, Zhao Y, Tsai C-C, Shen J, Bentley WE, Chen Y, Deng H, Du Y, Payne GF, Shi X (2018) Electrical writing onto a dynamically responsive polysaccharide medium: patterning structure and function into a reconfigurable medium. *Adv Struct Mater* 28:1803139
31. Rowe AA, Bonham AJ, White RJ, Zimmer MP, Yadgar RJ, Hobza TM, Honea JW, Ben-Yaacov I, Plaxco KW (2011) CheapStat: an open-source, “do-it-yourself” potentiostat for analytical and educational applications. *PLoS ONE* 6:e23783
32. Dryden MDM, Wheeler AR (2015) DStat: a versatile, open-source potentiostat for electroanalysis and integration. *PLoS ONE* 10:e0140349
33. Butterworth A, Corrigan DK, Ward AC (2019) Electrochemical detection of oxacillin resistance with SimpleStat: a low cost integrated potentiostat and sensor platform. *Anal Methods* 11:1958–1965
34. Ainla A, Mousavi MPS, Tsaloglou M-N, Redston J, Bell JG, Fernández-Abedul MT, Whitesides GM (2018) Open-source potentiostat for wireless electrochemical detection with smartphones. *Anal Chem* 90:6240–6246
35. Merceron TK, Murphy SV (2015) Chapter 14—hydrogels for 3D bioprinting applications. In: Atala A, Yoo JJ (eds) *Essentials of 3D biofabrication and translation*. Academic Press, Boston, pp 249–270
36. Yi H, Wu L-Q, Bentley WE, Ghodssi R, Rubloff GW, Culver JN, Payne GF (2005) Biofabrication with chitosan. *Biomacromolecules* 6:2881–2894
37. Maerten C, Jierry L, Schaaf P, Boulmedais F (2017) Review of electrochemically triggered macromolecular film buildup processes and their biomedical applications. *ACS Appl Mater Interfaces* 9:28117–28138
38. Kubiak PS, Awhida S, Hotchen C, Deng W, Alston B, McDonald TO, Adams DJ, Cameron PJ (2015) Polymerization of low molecular weight hydrogelators to form electrochromic polymers. *Chem Commun* 51:10427–10430
39. Groll J, Boland T, Blunk T, Burdick JA, Cho D-W, Dalton PD, Derby B, Forgacs G, Li Q, Mironov VA, Moroni L, Nakamura M, Shu W, Takeuchi S, Vozzi G, Woodfield TBF, Xu T, Yoo JJ, Malda J

- (2016) Biofabrication: reappraising the definition of an evolving field. *Biofabrication* 8:013001
40. Lei M, Qu X, Liu H, Liu Y, Wang S, Wu S, Bentley WE, Payne GF, Liu C (2019) Programmable electrofabrication of porous janus films with tunable janus balance for anisotropic cell guidance and tissue regeneration. *Adv Funct Mater* 29:1900065
 41. Gong J, Liu T, Song D, Zhang X, Zhang L (2009) One-step fabrication of three-dimensional porous calcium carbonate–chitosan composite film as the immobilization matrix of acetylcholinesterase and its biosensing on pesticide. *Electrochem Commun* 11:1873–1876
 42. Suginta W, Khunkaewla P, Schulte A (2013) Electrochemical biosensor applications of polysaccharides chitin and chitosan. *Chem Rev* 113:5458–5479
 43. Qi P, Wan Y, Zhang D (2013) Impedimetric biosensor based on cell-mediated bioimprinted films for bacterial detection. *Biosens Bioelectron* 39:282–288
 44. Ahuja T, Mir IA, Kumar D (2007) Biomolecular immobilization on conducting polymers for biosensing applications. *Biomaterials* 28:791–805
 45. Betz JF, Cheng Y, Tsao C-Y, Zargar A, Wu H-C, Luo X, Payne GF, Bentley WE, Rubloff GW (2013) Optically clear alginate hydrogels for spatially controlled cell entrapment and culture at microfluidic electrode surfaces. *Lab Chip* 13:1854–1858
 46. Xie C-M, Lu X, Wang K-F, Meng F-Z, Jiang O, Zhang H-P, Zhi W, Fang L-M (2014) Silver nanoparticles and growth factors incorporated hydroxyapatite coatings on metallic implant surfaces for enhancement of osteoinductivity and antibacterial properties. *ACS Appl Mater Interfaces* 6:8580–8589
 47. Thomas MB, Metoki N, Mandler D, Eliaz N (2016) In situ potentiostatic deposition of calcium phosphate with gentamicin-loaded chitosan nanoparticles on titanium alloy surfaces. *Electrochim Acta* 222:355–360
 48. Geuli O, Metoki N, Eliaz N, Mandler D (2016) Electrochemically driven hydroxyapatite nanoparticles coating of medical implants. *Adv Funct Mater* 26:8003–8010
 49. Chen Q, De Larraya UP, Garmendia N, Lasheras-Zubieta M, Cordero-Arias L, Virtanen S, Boccaccini AR (2014) Electrophoretic deposition of cellulose nanocrystals (CNS) and CNS/alginate nanocomposite coatings and free standing membranes. *Colloids Surf B* 118:41–48
 50. Patel KD, Singh RK, Lee E-J, Han C-M, Won J-E, Knowles JC, Kim H-W (2014) Tailoring solubility and drug release from electrophoretic deposited chitosan–gelatin films on titanium. *Surf Coat Technol* 242:232–236
 51. Wu L-Q, Gadre AP, Yi H, Kastantin MJ, Rubloff GW, Bentley WE, Payne GF, Ghodssi R (2002) Voltage-dependent assembly of the polysaccharide chitosan onto an electrode surface. *Langmuir* 18:8620–8625
 52. Brown DB, Rehmann D (2016) N chitosan biopolymer from fungal fermentation for delivery of chemotherapeutic agents. *Mater Mater* 11:86–89
 53. Gyles DA, Castro LD, Silva JOC, Ribeiro-Costa RM (2017) A review of the designs and prominent biomedical advances of natural and synthetic hydrogel formulations. *Eur Polym J* 88:373–392
 54. Thiele J, Ma Y, Bruekers SMC, Ma S, Huck WTS (2014) 25th anniversary article: designer hydrogels for cell cultures: a materials selection Guide. *Adv Mater* 26:125–148
 55. Draper ER, Adams DJ (2017) Low-molecular-weight gels: the state of the art. *Chem* 3:390–410
 56. Ghosh S, Praveen VK, Ajayaghosh A (2016) The chemistry and applications of π -gels. *Annu Rev Mater Res* 46:235–262
 57. Buerkle LE, Rowan SJ (2012) Supramolecular gels formed from multi-component low molecular weight species. *Chem Soc Rev* 41:6089–6102
 58. Adams DJ, Butler MF, Frith WJ, Kirkland M, Mullen L, Sanderson P (2009) A new method for maintaining homogeneity during liquid-hydrogel transitions using low molecular weight hydrogelators. *Soft Matter* 5:1856–1862
 59. Yan K, Xiong Y, Wu S, Bentley WE, Deng H, Du Y, Payne GF, Shi X-W (2016) Electro-molecular assembly: electrical writing of information into an erasable polysaccharide medium. *ACS Appl Mater Interfaces* 8:19780–19786
 60. Lakshminarayanan V, Poltorak L, Bosma D, Sudhölter EJR, Van Esch JH, Mendes E (2019) Locally pH controlled and directed growth of supramolecular gel microshapes using electrocatalytic nanoparticles. *Chem Commun* 55:9092–9095
 61. Gwon K, Kim M, Tae G (2014) A biocompatible method of controlled retrieval of cell-encapsulating microgels from a culture plate. *Integr Biol* 6:596–602
 62. Huang S-H, Wei L-S, Chu H-T, Jiang Y-L (2013) Light-addressed electrodeposition of enzyme-entrapped chitosan membranes for multiplexed enzyme-based bioassays using a digital micromirror device. *Sensors* 13:10711–10724
 63. Yan K, Liu Y, Zhang J, Correa SO, Shang W, Tsai C-C, Bentley WE, Shen J, Scarcelli G, Raub CB, Shi X-W, Payne GF (2018) Electrical programming of soft matter: using temporally varying electrical inputs to spatially control self assembly. *Biomacromolecules* 19:364–373
 64. Wang Y, Liu Y, Cheng Y, Kim E, Rubloff GW, Bentley WE, Payne GF (2011) Coupling electrodeposition with layer-by-layer assembly to address proteins within microfluidic channels. *Adv Mater* 23:5817–5821
 65. Leisk GG, Lo TJ, Yucel T, Lu Q, Kaplan DL (2010) Electrodeposition for protein adhesives. *Adv Mater* 22:711–715
 66. Liu Y, Kim E, Ulijn RV, Bentley WE, Payne GF (2011) Reversible electroaddressing of self-assembling amino-acid conjugates. *Adv Funct Mater* 21:1575–1580
 67. Li J, Maniar D, Qu X, Liu H, Tsao C-Y, Kim E, Bentley WE, Liu C, Payne GF (2019) Coupling self-assembly mechanisms to fabricate molecularly and electrically responsive films. *Biomacromolecules* 20:969–978
 68. Cross ER, Adams DJ (2019) Probing the self-assembled structures and pKa of hydrogels using electrochemical methods. *Soft Matter* 15:1522–1528
 69. Cross ER, Sproules S, Schweins R, Draper ER, Adams DJ (2018) Controlled tuning of the properties in optoelectronic self-sorted gels. *J Am Chem Soc* 140:8667–8670
 70. Rasband WS (1997–2018) ImageJ, U. S. National Institutes of Health, Bethesda, Maryland, USA. <https://imagej.nih.gov/ij/>. Accessed 20 Jan 2020
 71. Wallace M, Iggo JA, Adams DJ (2015) Using solution state NMR spectroscopy to probe NMR invisible gelators. *Soft Matter* 11:7739–7747
 72. Wallace M, Iggo JA, Adams DJ (2017) Probing the surface chemistry of self-assembled peptide hydrogels using solution-state NMR spectroscopy. *Soft Matter* 13:1716–1727
 73. Wallace M, Adams DJ, Iggo JA (2018) Titrations without the additions: the efficient determination of pKa values using NMR imaging techniques. *Anal Chem* 90:4160–4166
 74. Foster MP, Mcelroy CA, Amero CD (2007) Solution NMR of large molecules and assemblies. *Biochemistry* 46:331–340
 75. Draper ER, Lee JR, Wallace M, Jackel F, Cowan AJ, Adams DJ (2016) Self-sorted photoconductive xerogels. *Chem Sci* 7:6499–6505
 76. Weiss GR (2018) Controlling variables in molecular gel science: how can we improve the state of the art? *Gels* 4:25
 77. Mears LLE, Draper ER, Castilla AM, Su H, Zhuola Dietrich B, Nolan MC, Smith GN, Douth J, Rogers S, Akhtar R, Cui H, Adams DJ (2017) Drying affects the fiber network in low molecular weight hydrogels. *Biomacromolecules* 18:3531–3540

78. Draper ER, McDonald TO, Adams DJ (2015) A low molecular weight hydrogel with unusual gel aging. *Chem Commun* 51:6595–6597
79. Leal-Egaña A, Braumann U-D, Díaz-Cuenco A, Nowicki M, Bader A (2011) Determination of pore size distribution at the cell-hydrogel interface. *J Nanobiotechnol* 9:24
80. Nolan MC, Fuentes Caparrós AM, Dietrich B, Barrow M, Cross ER, Bleuel M, King SM, Adams DJ (2017) Optimising low molecular weight hydrogels for automated 3D printing. *Soft Matter* 13:8426–8432
81. Han F, Zhu C, Guo Q, Yang H, Li B (2016) Cellular modulation by the elasticity of biomaterials. *J Mater Chem B* 4:9–26
82. Anseth KS, Bowman CN, Brannon-Peppas L (1996) Mechanical properties of hydrogels and their experimental determination. *Biomaterials* 17:1647–1657

Publisher's Note Springer Nature remains neutral with regard to jurisdictional claims in published maps and institutional affiliations.